Journal of Scientific & Industrial Research
Vol. 82, July 2023, pp. 700-710
DOI: 10.56042/jsir.v82i07.1844

Addressing Model Uncertainties and External Disturbances in Optimal Robust Control for Vibration Reduction in a Flexible Link Manipulator

Sanjay Thakur* & Ranjit Kumar Barai

Department of Electrical Engineering, Jadavpur University, Kolkata 700 032, India

Received 04 October 2022; revised 23 May 2023; accepted 17 June 2023

A novel Optimal Robust Controller (ORC) for reducing vibration in a flexible link manipulator has been designed in this work. Compared to stiff link manipulators, flexible link manipulators have advantages, but they also have problems including link vibration, model uncertainty, and outside disruptions. The ORC aims to address these challenges and improve the positioning of the flexible links by reducing the link vibrations. Using the Assumed Mode Method (AMM), the dynamic model of a two-link flexible manipulator has been developed in order to create the ORC. With two mode shapes taken into consideration for each link, the deflection of the links has been modelled using mode shapes. The ORC has been designed to achieve robust performance in vibration reduction, even in the presence of unmatched model uncertainty. Proof of the matching condition of the uncertainty has been given, and the closed-loop stability of the resulting system has been established. The value of the uncertain parameter has been purposefully changed to illustrate the robustness of the created controller. For comparison purposes, a well-known reliable controller called the Sliding Mode Controller (SMC) has also been developed. The performance of the proposed ORC has been compared with that of the SMC in the simulation section, and the ORC is determined to be more effective at minimizing vibration.

Keywords: External disturbances, Matching condition, Payload, Sliding mode controller, Vibration

Introduction

The advantages of Flexible Link (FL) manipulators in comparison to rigid link manipulators have sparked a growing interest in their research. The links of the flexible link manipulator are light in weight. Hence high-rating actuators are not required. The flexible link manipulator's design cost and power needs are decreased by this capability. The light weight of the flexible link reduces stiffness. The prevalence of vibrations is a common and undesirable occurrence due to the low stiffness of the links. Since vibration degrades the system's performance and hinders the proper positioning of the links. FM might involve model uncertainty and external disruptions in addition to vibrations. Two-Link Flexible Manipulator (TLFM) is a highly nonlinear and coupled system too. Under such circumstances, the Optimal control approach alone is not sufficient and cannot perform well. Therefore, along with the Optimal controller, a robust controller can be used. Since, robust controllers can perform satisfactorily in the presence of incomplete dynamics, external disturbances, and model uncertainty also solving a robust problem using an optimal approach is simpler. To deal with such difficulties in this work Lin's approach[1] has been adopted. Apart from Lin's method, many control methods have also been developed for the control of FM such as robust control[2–7], observer-based control[8], sliding mode control[9–15], PD control[16], resonant control[17,18], etc. Since, Flexible manipulator is highly nonlinear and can have model uncertainties, external disturbance, vibrations, and incomplete information about the system dynamics. Under such conditions, robust controllers perform satisfactorily. Therefore, nowadays robust control methods are mostly adopted by researchers.

Wang *et al.*[5] introduced a robust H_∞ controller and conducted a comparative analysis with an LQR controller to assess their robustness and tracking precision. Lee & Lee[19] introduced variable structure control and virtual control force method to control joint angles and vibration of the links respectively. Hisseine & Lohmann[2] compared the performance of sliding mode control and nonlinear H_∞ control techniques for the flexible manipulator. It has been found that the sliding mode technique works well in the presence of pant uncertainties due to parameter variations. For joint location tracking and vibration reduction in the face of model uncertainty, SMC has

*Author for Correspondence
E-mail: sanjaythakur.ee.rs@jadavpuruniversity.in

been designed by Thakur & Barai.[14] Variations in the value of the uncertain parameter, equivalent viscous damping, have been made. A comparative analysis was conducted to evaluate the performance of the controller in comparison with the Proportional-Derivative (PD) controller. Thakur *et al.*[20] proposed a Lyapunov-based controller for vibration reduction. Model uncertainty (equivalent viscous damping coefficient) has been considered by the author. A Crow search algorithm has been developed by the author to control the link vibration in an optimal way.[21] Sasaki *et al.*[22] combined three control logics i.e., feed forward controller, adaptive notch filter and strain feedback controller, to effectively mitigate vibrations in the flexible links. To overcome the vibration problem Abdul-Lateef *et al.*[23] proposed a controller that has been designed by the author by combining the neural network with broad learning theory. Karkoub *et al.*[24] proposed a linearized model with model uncertainty and a robust controller has been designed for tip trajectory tracking. Daafouz *et al.*[7], varied the payload to show the performance of the robust controller designed by solving a two-variable Riccati equation. Along with trajectory tracking, the collision problem has been addressed by Morlock *et al*.[25] Using variable structure controllers like SMC, the chattering problem in the controller response is normal. To overcome this problem, He *et al.*[26] integrated a neural network into the back-stepping method and its effectiveness has been compared with a PD controller. Some authors divide the FM system into two subsystems, slow mode (rigid components) and fast mode (flexible components).[4,27,28] For vibration reduction, the slow mode utilizes SMC (Sliding Mode Control), while the fast mode employs the Linear Quadratic Regulator (LQR) controller. [27,28] To improve control performance, Li *et al.*[4] created a decomposition-based robust controller and different controllers for the slow and fast subsystems. Mathematical model of flexible manipulator has been obtained by different modeling approaches such as finite element method[29,30], assumed mode method[9,31–33], and lumped parameter method.[34–36] Each method has its own pros and cons.

From the above-mentioned references, it is clear that the robust controllers have been mostly used by researchers and the link vibration is the major obstacle that is required to overcome before performing any task. Most of the controllers that have been proposed previously contain unknown gains. For the proper tuning of those gains, some extra methods need to be incorporated with the existing controller. The use of extra tuning methods increases the computational burden on the controllers. To overcome such issues, in this work, an Optimal robust controller has been developed which does not contain any unknown gains, in the frame proposed by Lin[1]. The robust control problem was initially formulated using model uncertainty and vibration. Then that robust control problem has been solved in an optimal way. Because, the solution derived from the optimal control problem can also be utilized as a solution for the robust control problem.[1] Some notable features of the presented work include: i) The proposed controller is free of unknown terms, eliminating the need for additional tuning methods. ii) To date, no researchers have utilized Lin's method for vibration reduction in a two-link flexible manipulator, making it a novel contribution. iii) Model uncertainty, specifically the payload, has been taken into account, and proof of the matching condition has been provided.

Here, the dynamics of TLFM have been obtained using AMM considering two modes for each link. External disturbances and model uncertainty have been taken into account. Evidence of the matching condition for the model uncertainty, specifically the payload mass, has been provided. Since the matching condition plays a major role in the design of the controller. The mass of the payload has been seen as a source of uncertainty. Because any change in its value can have a significant impact on the system's performance. To show the reliability of the suggested Optimal Robust Controller (ORC), the value of the uncertain parameter has been changed in this problem. In the simulation section, a comparative evaluation has been conducted between the developed Optimal Robust Controller (ORC) and a Sliding Mode Controller (SMC), revealing superior performance of the ORC.

Modeling and Problem Formulation of TLFM

In Fig. 1, it has been shown that motor1 is connected at the base. M_1 represent the mass of the second motor which connects link1 and link2 and M_2 represents the mass of the payload attached at the free end of link2. w and θ are the deflection and angular position of the flexible links respectively. δ_{11}, δ_{12} are the mode shapes associated with the link1 and δ_{22}, δ_{21} are the mode shapes associated with link2. σ_1 and σ_2

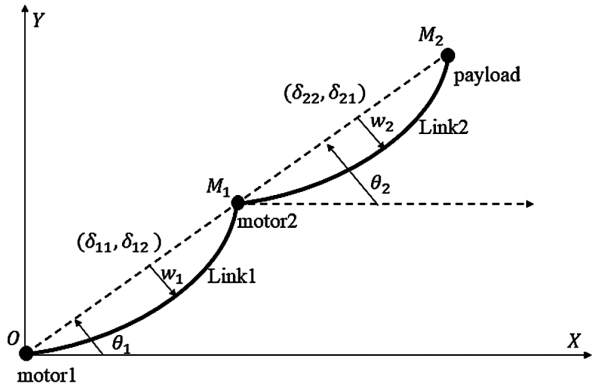

Fig. 1 — Planer TLFM (inspired from Yang and Zhong[37])

are the mass of link1 and link2 respectively. In this work, the attachment of flexible links has been implemented using Revolute joints, enabling the links to move exclusively within the horizontal plane. The primary focus was to maintain a collision-free environment for the two-link flexible manipulator, as collisions could cause damage to both its physical structure and operational capability. Furthermore, altering the cross-section of the link would result in a significant modification of the overall dynamics. Additionally, the dynamic model presented in the paper would undergo changes if the influence of gravity were to be taken into consideration. Hence, before designing the controllers, some assumptions have been made: (i) The motion of the TLFM has been restricted in the horizontal plane, (ii) the Gravity effect has been ignored, (iii) There is no collision point in the workspace of the TLFM, (iv) Throughout the operation, the cross-section of the flexible links remains constant. With the help of these assumptions, the dynamics of the TLFM have been given as[37]

$$\begin{bmatrix} \mathrm{M}_{\Theta\Theta} & \mathrm{M}_{\Theta\delta} \\ \mathrm{M}_{\delta\Theta} & \mathrm{M}_{\delta\delta} \end{bmatrix} \begin{bmatrix} \ddot{Q}_{\Theta} \\ \ddot{Q}_{\delta} \end{bmatrix} + \begin{bmatrix} \varsigma_{\Theta} \\ \varsigma_{\delta} \end{bmatrix} + \begin{bmatrix} 0 & 0 \\ 0 & \Re \end{bmatrix} \begin{bmatrix} Q_{\Theta} \\ Q_{\delta} \end{bmatrix} = \begin{bmatrix} \Im_{\Theta} \\ 0 \end{bmatrix} \Im$$

$$\Im_{\Theta} = \left(\mathrm{M}_{\Theta\Theta} - \mathrm{M}_{\Theta\delta}\mathrm{M}_{\delta\delta}^{-1}\mathrm{M}_{\delta\Theta}\right)\ddot{Q}_{\Theta} - \mathrm{M}_{\Theta\delta}\mathrm{M}_{\delta\delta}^{-1}\left(\varsigma_{\delta} + \Re Q_{\delta}\right) + \varsigma_{\Theta} \quad \ldots (1)$$

where, Coriolis-centrifugal forces acting on the system are given by the matrix $\begin{bmatrix} \varsigma_{\theta} & \varsigma_{\delta} \end{bmatrix}^T$, $\Im_{\theta} = \begin{bmatrix} T_1 & T_2 \end{bmatrix}^T$ is the control torque, T_1 is the torque of the Motor1, T_2 is the torque of the Motor2, $\Re$ is the stiffness matrix, and $\begin{bmatrix} \mathrm{M}_{\Theta\Theta} & \mathrm{M}_{\Theta\delta} \\ \mathrm{M}_{\delta\Theta} & \mathrm{M}_{\delta\delta} \end{bmatrix}$ is the inertia matrix of the entire system. Detailed expressions have been presented as[37]

$$\Re = diag\left(A_1, A_2, A_3, A_4\right)$$

$$A_1 = \frac{\pi^4}{2\ell_1^3}\xi_1, A_2 = \frac{8\pi^4}{\ell_1^3}\xi_1, A_3 = \frac{\pi^4}{2\ell_2^3}\xi_2, A_4 = \frac{8\pi^4}{\ell_2^3}\xi_2$$

The expressions of the inertia matrix can be given as [37]-

$$\mathrm{M}_{\Theta\Theta} = \begin{bmatrix} \Theta_{11} & \Theta_{12} \\ \Theta_{21} & \Theta_{22} \end{bmatrix}; \mathrm{M}_{\Theta\delta} = \begin{bmatrix} \Theta_{13} & \Theta_{14} & \Theta_{15} & 0 \\ 0 & 0 & \Theta_{25} & \Theta_{26} \end{bmatrix}; \mathrm{M}_{\delta\Theta}$$

$$= \begin{bmatrix} \Theta_{31} & 0 \\ \Theta_{41} & 0 \\ \Theta_{51} & \Theta_{52} \\ 0 & \Theta_{62} \end{bmatrix}; \mathrm{M}_{\delta\delta} = \begin{bmatrix} \Theta_{33} & 0 & 0 & 0 \\ 0 & \Theta_{44} & 0 & 0 \\ 0 & 0 & \Theta_{55} & 0 \\ 0 & 0 & 0 & \Theta_{66} \end{bmatrix},$$

$$\theta_{12} = \left(\theta_1 - \theta_2\right)$$

$$\Theta_{11} = \left(\frac{1}{3}\sigma_1 + \sigma_2 + \mathrm{M}_1 + \mathrm{M}_2\right)\ell_1^2 + \frac{1}{2}\sigma_1\left(\delta_{11}^2 + \delta_{12}^2\right), \Theta_{12} = \Theta_{21}$$

$$= \left(\frac{1}{2}\sigma_1 + \mathrm{M}_1\right)\ell_1\ell_2\cos\left(\theta_{12}\right) + \frac{2}{\pi}\sigma_2\ell_1\delta_{21}\sin\left(\theta_{12}\right),$$

$$\Theta_{13} = \Theta_{31} = -\frac{1}{\pi}\sigma_1\ell_1, \Theta_{14} = \Theta_{41} = \frac{1}{2\pi}\sigma_1\ell_1, \Theta_{15} = \Theta_{51}$$

$$= \frac{2}{\pi}\sigma_2\ell_1\cos\left(\theta_{12}\right), \Theta_{22} = \left(\frac{1}{3}\sigma_2 + \mathrm{M}_2\right)\ell_2^2 + \frac{1}{2}\sigma_2\left(\delta_{11}^2 + \delta_{12}^2\right),$$

$$\Theta_{25} = \Theta_{52} = \frac{1}{\pi}\sigma_2\ell_2, \Theta_{26} = \Theta_{62} = -\frac{1}{2\pi}\sigma_2\ell_2, \Theta_{33}$$

$$= \frac{1}{2}\sigma_1, \Theta_{44} = \frac{1}{2}\sigma_1, \Theta_{55} = \frac{1}{2}\sigma_2, \Theta_{66} = \frac{1}{2}\sigma_2.$$

The detailed expression for Coriolis-centrifugal force can be given as [37]-

$$\varsigma_{\Theta} = \begin{bmatrix} c_1 & c_2 \end{bmatrix}^T, \varsigma_{\delta} = \begin{bmatrix} c_3 & c_4 & c_5 & c_6 \end{bmatrix}^T$$

$$c_1 = \frac{1}{2}\left(\sigma_1 - \sigma_2\right)\ell_1\ell_2\dot{\theta}_1\dot{\theta}_2\sin\theta_{12} + \frac{1}{2}\left(\sigma_1 + \mathrm{M}_2\right)\ell_1\ell_2\dot{\theta}_2^2\sin\theta_{12}$$

$$+\frac{4}{\pi}\sigma_2\ell_1\dot{\theta}_2\dot{\delta}_{21}\sin\theta_{12} - \frac{2}{\pi}\sigma_2\ell_1\delta_{21}\dot{\theta}_2^2\cos\theta_{12} + \sigma_1\delta_{11}\dot{\theta}_1\dot{\delta}_{11} + \sigma_1\delta_{12}\dot{\theta}_1\dot{\delta}_{12},$$

$$c_2 = -\frac{1}{2}\left(\sigma_2 + \mathrm{M}_2\right)\ell_1\ell_2\dot{\theta}_1^2\sin\theta_{12} + \frac{2}{\pi}\sigma_2\ell_1\delta_{21}\dot{\theta}_1^2\cos\theta_{12}$$

$$+\sigma_2\delta_{21}\dot{\theta}_2\dot{\delta}_{21} + \sigma_2\delta_{22}\dot{\theta}_2\dot{\delta}_{22}, c_3 = -\frac{1}{2}\sigma_1\delta_{11}\dot{\theta}_1,$$

$$c_4 = -\frac{1}{2}\sigma_1\delta_{12}\dot{\theta}_1, c_5 = -\frac{2}{\pi}\sigma_2\ell_1\dot{\theta}_1^2\sin\theta_{12} - \frac{1}{2}\sigma_2\delta_{21}\dot{\theta}_2^2,$$

$$c_6 = -\frac{1}{2}\sigma_2\delta_{22}\dot{\theta}_2$$

Before proving the matching condition of the uncertain value some assumptions are made: a) deflections are neglected, b) joint angles are considered very small. Let, M_2 be the uncertain value

a) deflections are neglected, b) joint angles are considered very small. Let, M_2 be the uncertain value of the payload and M_{20} be the nominal value of the payload. The Eq. (1). can also be rewritten as

$$\ddot{Q}_\Theta = -\left(\mathrm{M}_{\Theta\Theta} - \mathrm{M}_{\Theta\delta}\mathrm{M}_{\delta\delta}^{-1}\mathrm{M}_{\delta\Theta}\right)^{-1}\left(\varsigma_\Theta - \mathrm{M}_{\Theta\delta}\mathrm{M}_{\delta\delta}^{-1}\left(\varsigma_\delta + \Re\ddot{Q}_\delta\right)\right) + \left(\mathrm{M}_{\Theta\Theta} - \mathrm{M}_{\Theta\delta}\mathrm{M}_{\delta\Theta}^{-1}\mathrm{M}_{\delta\Theta}\right)^{-1}\Im_\Theta + d_{ex} \quad \ldots (2)$$

where, d_{ex} is the external disturbance. Let's calculate each term without considering external disturbance and using the assumptions made for the matching condition and using the parameter values given in Table 1.

Part 1-

$$\left(\mathrm{M}_{\Theta\Theta} - \mathrm{M}_{\Theta\delta}\mathrm{M}_{\delta\delta}^{-1}\mathrm{M}_{\delta\Theta}\right)^{-1} = \chi_{(\mathrm{M}_2)}\begin{pmatrix} 0.1601+\mathrm{M}_2 & -0.989431 \\ -0.989431 & 1.339+\mathrm{M}_2 \end{pmatrix} \quad \ldots (3)$$

where, $\chi_{(\mathrm{M}_2)} = \dfrac{1}{\mathrm{M}_2^2 + 1.4991\mathrm{M}_2 - 0.7645}$.

Part 2-

$$\left(\varsigma_\Theta - \mathrm{M}_{\Theta\delta}\mathrm{M}_{\delta\delta}^{-1}\left(\varsigma_\delta + \Re Q_\delta\right)\right) = \begin{pmatrix} \frac{1}{2}\left(2+\mathrm{M}_2\right)\dot{\theta}_2^2\sin\theta_{12} + 0.8106\dot{\theta}_1^2\sin\theta_{12} \\ -\frac{1}{2}\left(2+\mathrm{M}_2\right)\dot{\theta}_1^2\sin\theta_{12} + 0.8106\dot{\theta}_1^2\sin\theta_{12} \end{pmatrix} \quad \ldots (4)$$

Let, the speed of rotation of the joints is limited by

$$\left.\begin{matrix} \|\dot{\theta}_1\| \\ \|\dot{\theta}_2\| \end{matrix}\right\} \leq \Psi \quad \ldots (5)$$

where, Ψ is a positive integer. Combining Eqs (4 & 5) can be expressed as

$$\left(\varsigma_\Theta - \mathrm{M}_{\Theta\delta}\mathrm{M}_{\delta\delta}^{-1}\left(\varsigma_\delta + \Re Q_\delta\right)\right) \leq \theta_{12}\Psi\begin{pmatrix} 0.8106 & 1+0.5\mathrm{M}_2 \\ -0.1894-0.5\mathrm{M}_2 & 0 \end{pmatrix}\begin{pmatrix} \dot{\theta}_1 \\ \dot{\theta}_2 \end{pmatrix} \quad \ldots (6)$$

Part 3-

$$\left(\mathrm{M}_{\Theta\Theta} - \mathrm{M}_{\Theta\delta}\mathrm{M}_{\delta\delta}^{-1}\mathrm{M}_{\delta\Theta}\right)^{-1}\left(\varsigma_\Theta - \mathrm{M}_{\Theta\delta}\mathrm{M}_{\delta\delta}^{-1}\left(\varsigma_\delta + \Re Q_\delta\right)\right) \leq \chi_{(\mathrm{M}_2)}\theta_{12}\Psi\hbar_{(\mathrm{M}_2)}\begin{pmatrix} \dot{\theta}_1 \\ \dot{\theta}_2 \end{pmatrix} \quad \ldots (7)$$

where,

$$\hbar_{(\mathrm{M}_2)} = \begin{pmatrix} 0.31718+1.30532\mathrm{M}_2 & 0.1601+1.5\mathrm{M}_2 \\ -1.05564-0.85890\mathrm{M}_2 & -0.98943-0.49472\mathrm{M}_2 \end{pmatrix}$$

Eq. (7) can also be written for M_{20}

$$\left(\mathrm{M}_{\Theta\Theta} - \mathrm{M}_{\Theta\delta}\mathrm{M}_{\delta\delta}^{-1}\mathrm{M}_{\delta\Theta}\right)^{-1}\begin{pmatrix} \varsigma_\Theta - \mathrm{M}_{\Theta\delta}\mathrm{M}_{\delta\delta}^{-1} \\ \left(\varsigma_\delta + \Re Q_\delta\right) \end{pmatrix} \leq \chi_{(\mathrm{M}_{20})}\theta_{12}\Psi\hbar_{(\mathrm{M}_{20})}\begin{pmatrix} \dot{\theta}_1 \\ \dot{\theta}_2 \end{pmatrix} \quad \ldots (8)$$

Eq. (2) can be written as

$$\ddot{Q}_\Theta = \hat{A} + \hat{B}\Im_\Theta \quad \ldots (9)$$

It can be observed that the matrix $\hat{A}$ and $\hat{B}$ both contain the uncertain parameter. Please note

$$\hat{A}\left(\mathrm{M}_2\right) = -\chi_{(\mathrm{M}_2)}\theta_{12}\Psi\hbar_{(\mathrm{M}_2)}\begin{pmatrix} \dot{\theta}_1 \\ \dot{\theta}_2 \end{pmatrix}$$
$$\hat{B} = \left(\mathrm{M}_{\Theta\Theta} - \mathrm{M}_{\Theta\delta}\mathrm{M}_{\delta\delta}^{-1}\mathrm{M}_{\delta\Theta}\right)^{-1} \quad \ldots (10)$$

$$\hat{A}\left(\mathrm{M}_{20}\right) = -\chi_{(\mathrm{M}_{20})}\theta_{12}\Psi\hbar_{(\mathrm{M}_{20})}\begin{pmatrix} \dot{\theta}_1 \\ \dot{\theta}_2 \end{pmatrix} \quad \ldots (11)$$

Therefore, it can be observed that

$$\hat{A}\left(\mathrm{M}_2\right) - \hat{A}\left(\mathrm{M}_{20}\right) \neq \hat{R}\hat{B} \quad \ldots (12)$$

where, $\hat{R}$ is a nonzero quantity. The analysis of Eq. (12), reveals that the uncertainty lies outside the range $\hat{B}$. As a result, the model uncertainty, introduced into the system through the input matrix $\hat{B}$, fails to meet the matching condition.

Controller Design

In this section, first, the robust control problem has been discussed and formulated. Then this problem has been solved using the Optimal approach. The Optimal robust controller has been designed without considering external disturbance.

Optimal Robust Controller (ORC) Design

It is observed from the previous section that, the input matrix and system matrix both consist of an uncertain parameter. At first, the robust control problem has been constructed considering uncertainty then this robust control problem has been solved using an optimal control approach.

Robust Control Problem

Eq. (9) can be rewritten as

$$\dot{\Omega} = \Upsilon(\rho)\Omega + \mathrm{B}\Lambda(\rho)\varphi \quad \ldots (13)$$

The uncertainty matrix, denoted as $\Lambda(\rho)$, represents the level of uncertainty within the input matrix and $0 < \Lambda \leq \Lambda(\rho)$. Assume the presence of a nominal value $\rho_0 \in \rho$ associated with ρ, such that $\left(\Upsilon(\rho_0), B\right)$ is stabilized. The objective is to find a

feedback control law $\varphi = \varphi_0$, such that the closed-loop system Eq. (13) would be asymptotically stable. The uncertainty in the system matrix has been represented as[1]

$$\Upsilon(\rho) - \Upsilon(\rho_0) = (\mathrm{B}\Lambda)(\mathrm{B}\Lambda)^{+}\left(\Upsilon(\rho) - \Upsilon(\rho_0)\right) + \left(\dagger - (\mathrm{B}\Lambda)(\mathrm{B}\Lambda)^{+}\right)\left(\Upsilon(\rho) - \Upsilon(\rho_0)\right) \quad \ldots (14)$$

where, $(\mathrm{B}\Lambda)^{+}$ is the pseudo inverse of $(\mathrm{B}\Lambda)$ and $\dagger$ is the identity matrix. With the help of a pseudo-inverse matrix, the auxiliary system equation can be given as

$$\dot{\Omega} = \Upsilon(\rho_0)\Omega + \mathrm{B}\Lambda\varphi + \left(\dagger - (\mathrm{B}\Lambda)(\mathrm{B}\Lambda)^{+}\right)\vartheta \quad \ldots (15)$$

ϑ is the added controller which is used to deal with the system's uncertainty.

Optimal Control Problem

The goal is to discover a feedback control law $(\varphi_0 = k\Omega, \vartheta_0 = \lambda\Omega)$ that effectively minimizes the given cost function.[1]

$$\int_0^{\infty}\left(\Omega^T(G + H + \dagger)\Omega + \varphi\varphi^T + \vartheta\vartheta^T\right)dt \quad \ldots (16)$$

where,

$$G \geq \left\|(\mathrm{B}\Lambda)^{+}\left(\Upsilon(\rho) - \Upsilon(\rho_0)\right)\right\|$$
$$H \geq \left\|\left(\Upsilon(\rho) - \Upsilon(\rho_0)\right)\right\| \quad \ldots (17)$$

Since the solution of the optimal control problem serves as a solution to the robust control problem, hence the solution to the robust control problem will be represented by $(\varphi_0(\Omega), \vartheta_0(\Omega))$. Therefore, the goal of $(\varphi_0(\Omega), \vartheta_0(\Omega))$ is to make the Eq. (15) asymptotically stable.

Proof of Stability

Proof of $(\varphi_0(\Omega), \vartheta_0(\Omega))$, making the auxiliary system asymptotically stable has been presented below.

Let's define

$$V(\Omega_0) = \min\int_0^{\infty}\left(\Omega^T(G + H + \dagger)\Omega + \varphi\varphi^T + vv^T\right)dt \quad \ldots (18)$$

Table 1 — TLFM parameters[37]

	Link1	Link2
Length of the link	$\ell_1 = 1.0\ (m)$	$\ell_2 = 1.0\ (m)$
Mass of the link	$\sigma_1 = 2.0\ (kg)$	$\sigma_2 = 2.0\ (kg)$
Motor mass and Payload mass	$\mathrm{M}_1 = 0.8\ (kg)$	$\mathrm{M}_2 = 0.5\ (kg)$
Flexural rigidity of the links	$\xi_1 = 2.0\,(N.m^2)$	$\xi_2 = 2.0\,(N.m^2)$

For $V(\Omega_0)$, to be asymptotically stable, it has to satisfy the Hamilton – Jacobi – Bellman equation[1] for some initial value Ω_0, which reduced to

$$\min\left(\Omega^T(G + H + \dagger)\Omega + \varphi\varphi^T + \vartheta\vartheta^T\right) + V_{\Omega}^T\begin{pmatrix}\Upsilon(\rho_0)\Omega + \mathrm{B}\Lambda\varphi \\ +\left(\dagger - (\mathrm{B}\Lambda)(\mathrm{B}\Lambda)^{+}\right)\vartheta\end{pmatrix} = 0$$
$$2\varphi + V_{\Omega}^T\mathrm{B}\Lambda = 0 \quad \ldots (19)$$
$$2\vartheta + V_{\Omega}^T\left(\dagger - (\mathrm{B}\Lambda)(\mathrm{B}\Lambda)^{+}\right) = 0$$

where, $V_{\Omega}^T = \frac{\partial V}{\partial \Omega}$. To show $\dot{V}(\Omega) < 0$ for all $\Omega \neq 0$, a Lyapunov candidate function has been considered, mentioned bellow

$$\dot{V}(\Omega) = V_{\Omega}^T\dot{\Omega} = V_{\Omega}^T\left(\Upsilon(\rho)\Omega + \mathrm{B}\Lambda(\rho)\varphi\right)$$
$$= -\Omega^T(G + H + \dagger)\Omega - \varphi\varphi^T - \vartheta\vartheta^T + V_{\Omega}^T\left(\Upsilon(\rho) - \Upsilon(\rho_0)\right)$$
$$\Omega - V_{\Omega}^T\left(\dagger - (\mathrm{B}\Lambda)(\mathrm{B}\Lambda)^{+}\right)\vartheta \quad \ldots (20)$$

Using Eq. (19), let's calculate each term separately,

Term1-

$$V_{\Omega}^T\left(\Upsilon(\rho) - \Upsilon(\rho_0)\right)\Omega = -2\varphi(\mathrm{B}\Lambda)^{+}$$
$$\left(\Upsilon(\rho) - \Upsilon(\rho_0)\right) - 2\vartheta\left(\Upsilon(\rho) - \Upsilon(\rho_0)\right)\Omega \quad \ldots (21)$$

Term2-

$$V_{\Omega}^T\left(\dagger - (\mathrm{B}\Lambda)(\mathrm{B}\Lambda)^{+}\right)\vartheta = -2\vartheta^T\vartheta \quad \ldots (22)$$

Putting Eq. (21) and Eq. (22) in Eq. (20),

$$\dot{V}(\Omega) = -\Omega^T(G + H + \dagger)\Omega - \varphi\varphi^T - \vartheta\vartheta^T$$
$$-2\varphi(\mathrm{B}\Lambda)^{+}\left(\Upsilon(\rho) - \Upsilon(\rho_0)\right) \quad \ldots (23)$$
$$-2\vartheta\left(\Upsilon(\rho) - \Upsilon(\rho_0)\right)\Omega + 2\vartheta^T\vartheta$$

Again, some terms have been separately calculated,

$$-\vartheta\vartheta^T - 2\vartheta\left(\Upsilon(\rho) - \Upsilon(\rho_0)\right)\Omega + 2\vartheta^T\vartheta \leq \Omega^T H\Omega + 2\vartheta^T\vartheta \quad \ldots (24)$$

$$-\varphi\varphi^T - 2\varphi(\mathrm{B}\Lambda)^{+}\left(\Upsilon(\rho) - \Upsilon(\rho_0)\right) \leq \Omega^T G\Omega \quad \ldots (25)$$

Putting Eq. (24) and Eq. (25) in Eq. (23),

$$\dot{V}(\Omega) \leq -\Omega^T\Omega + 2\vartheta^T\vartheta \quad \ldots (26)$$

Therefore, Eq. (26) can be written as,

$$\dot{V}(\Omega) \leq -\Omega^T\left(\dagger - 2\lambda^T\lambda\right)\Omega \quad \ldots (27)$$

From Eq. (27), it is evident that if the necessary condition $\left(\dagger - 2\lambda^T\lambda\right) > 0$ is fulfilled, then

$$\dot{V}(\Omega) < 0 \quad \Omega \neq 0$$
$$\dot{V}(\Omega) = 0 \quad \Omega = 0 \quad \ldots (28)$$

As a result, the system achieves stability, proving to be the answer to the challenge of robust control.

Sliding Mode Controller (SMC) Design

For comparison purposes, a popular robust controller i.e., sliding mode controller has been designed using the sliding surface, defined as $S = \dot{Q}_\Theta + \lambda Q_\Theta$.[38] The sliding condition has been considered as $\frac{1}{2}\frac{d}{dt}S^2 \le -\eta|S|$.[38] Where, λ and η are strictly positive constant. A very simple design procedure has been adopted considering a traditional sliding surface. SMC has been designed without considering external disturbance. The sliding surface is the most important part of the SMC design. In this work, a very traditional sliding surface has been considered[38], given as

$$S = \dot{Q}_\Theta + \lambda Q_\Theta \qquad \ldots (29)$$

where, λ is a positive quantity. Using Eq. (29), Eq.(2) and the signum function $(\mathrm{sgn}(*))$, the controller expression has been presented as

$$\Im_\Theta = H^{-1}\left(\ddot{Q}_{\Theta d} - \lambda\dot{e} - \mathrm{M}_2 S + H\varsigma_\Theta - HH_1 - \eta\,\mathrm{sgn}(S)\right) \qquad \ldots (30)$$

where, $H = \left(\mathrm{M}_{\Theta\Theta} - \mathrm{M}_{\Theta\delta}\mathrm{M}_{\delta\delta}^{-1}\mathrm{M}_{\delta\Theta}\right)^{-1}$,

$H_1 = \mathrm{M}_{\Theta\delta}\mathrm{M}_{\delta\delta}^{-1}\left(\varsigma_\delta + \Re Q_\delta\right)$ and $\eta \ge 0$.

Stability Proof-

The Lyapunov function can be considered as,

$$V = \frac{1}{2}S^T S \qquad \ldots (31)$$

Taking the derivative of Eq. (31),

$$\begin{aligned}\dot{V} &= S^T\dot{S}\\ &= S^T\left(\ddot{Q}_\Theta + \lambda\dot{Q}_\Theta\right) \qquad \ldots (32)\\ &= S^T\lambda\dot{Q}_\Theta + S^T\left(HH_1 - H\varsigma_\Theta + H\Im_\Theta\right)\end{aligned}$$

Using Eqs. (30 & 32),

$$\dot{V} = -S^T\eta\,\mathrm{sgn}(S) - S^T\mathrm{M}_2 S \qquad \ldots (33)$$

where, $\mathrm{M}_2 > 0$ and $\eta \ge 0$. Therefore, from Eq. (33) it can be observed that $\dot{V} \le 0$. As a result, the Lyapunov stability requirement has been met.

Simulation Results and Discussion

The simulation results in this section were produced utilising newly developed controllers. The simulation was conducted in MATLAB, utilizing the RK method with a time step of 0.001 seconds. The simulation has been run for 100 seconds to present more informative results. The Two-Link Flexible Manipulator (TLFM) parameter values are given in Table 1. External disturbance d_{ex} has been considered as 0.02.[37] The value of the constants λ and η used in the Sliding Mode Controller (SMC) design are 1.5 and 0.3 respectively. Ψ has been considered as 10 which indicates that the speed of the rotation of the flexible link has been limited by 10. The simulation results have been obtained by varying the uncertain parameter value. Let, $\mathrm{M}_{20} = 10$ and the value of M_2 has been varied as 3, 7, and 10. The initial value of the state has been considered as $\left(\theta_1, \dot{\theta}_1, \theta_2, \dot{\theta}_2\right) = \left(0.1, 0.01, 0.2, 0.02\right)$.

The conditions where the payload mass (uncertainty) has been taken as 3 kg are shown in Figs 2 & 3. The amplitude of maximum deflection of the mode functions $\left(\delta_{11\max}, \delta_{12\max}, \delta_{21\max}, \delta_{22\max}\right)$ is very less in the case of the proposed Optimal Robust Controller (ORC) than SMC. It can also be noticed that the maximum torque needed by the joint actuators $\left(T_{1\max}\right)$ and $\left(T_{2\max}\right)$ is $0.4179\ N.m$ and $0.1682\ N.m$

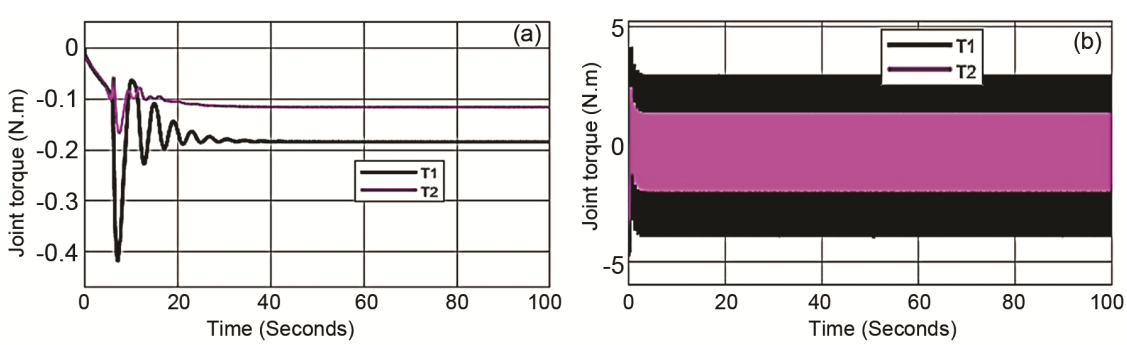

Fig. 2 — Control torque response of the joint actuators for $M_2 = 3\ kg$; Results obtained using: (a) Optimal robust controller and (b) Sliding mode controller

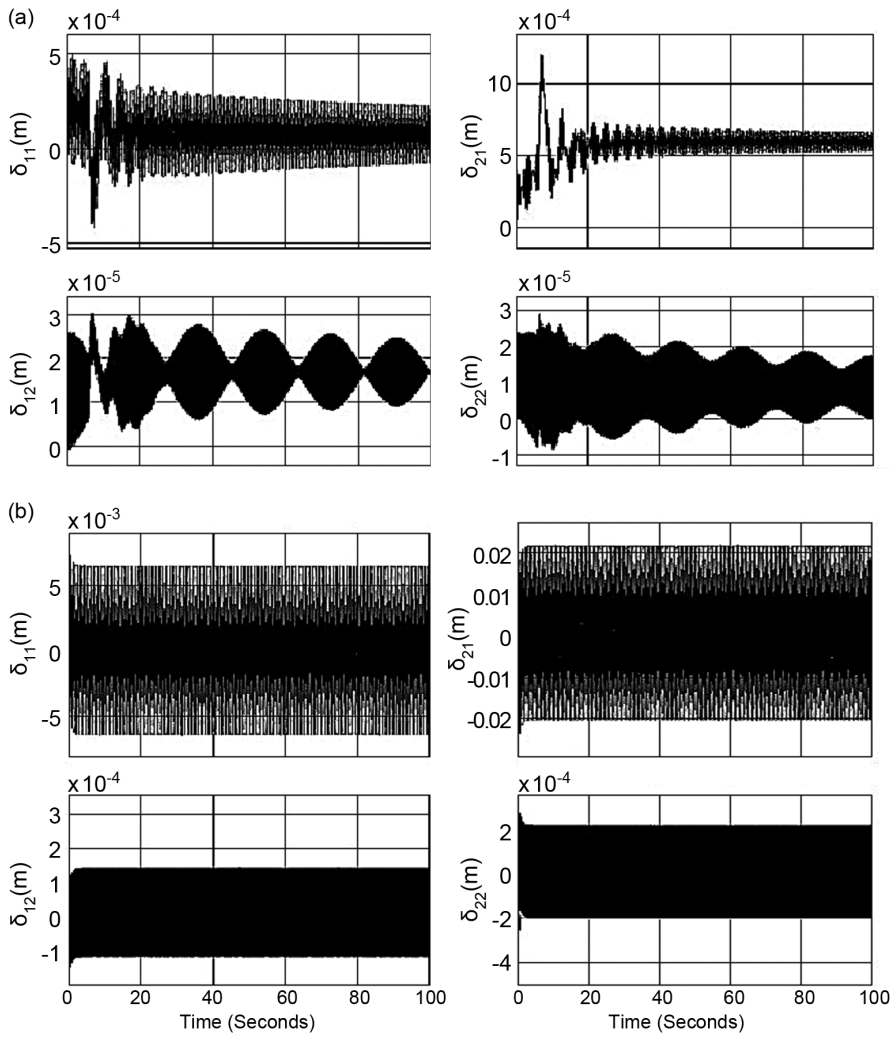

Fig. 3 — Modal function response, δ_{11} and δ_{12} are the modal function of Link 1 whereas δ_{21} and δ_{22} are the modal function of Link2, when payload is $M_2 = 3\ kg$; Results obtained using: (a) Optimal robust controller and (b) Sliding mode controller

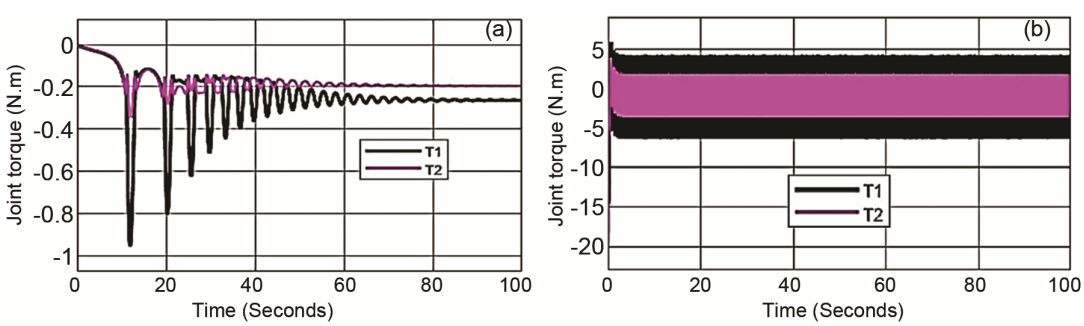

Fig. 4 — Control torque response of the joint actuators for $M_2 = 7\ kg$; Results obtained using: (a) Optimal robust controller and (b) Sliding mode controller

respectively in the case of the proposed optimal robust controller, whereas the maximum torque needed by the actuators is $T_{1\max} = 4.722\ N.m$ and $T_{1\max} = 4.848\ N.m$ in the case of the sliding mode controller. The less value of the torque puts less burden on the controllers and very high rating actuators are not required, which reduces the design cost and power consumption. The scenario with the

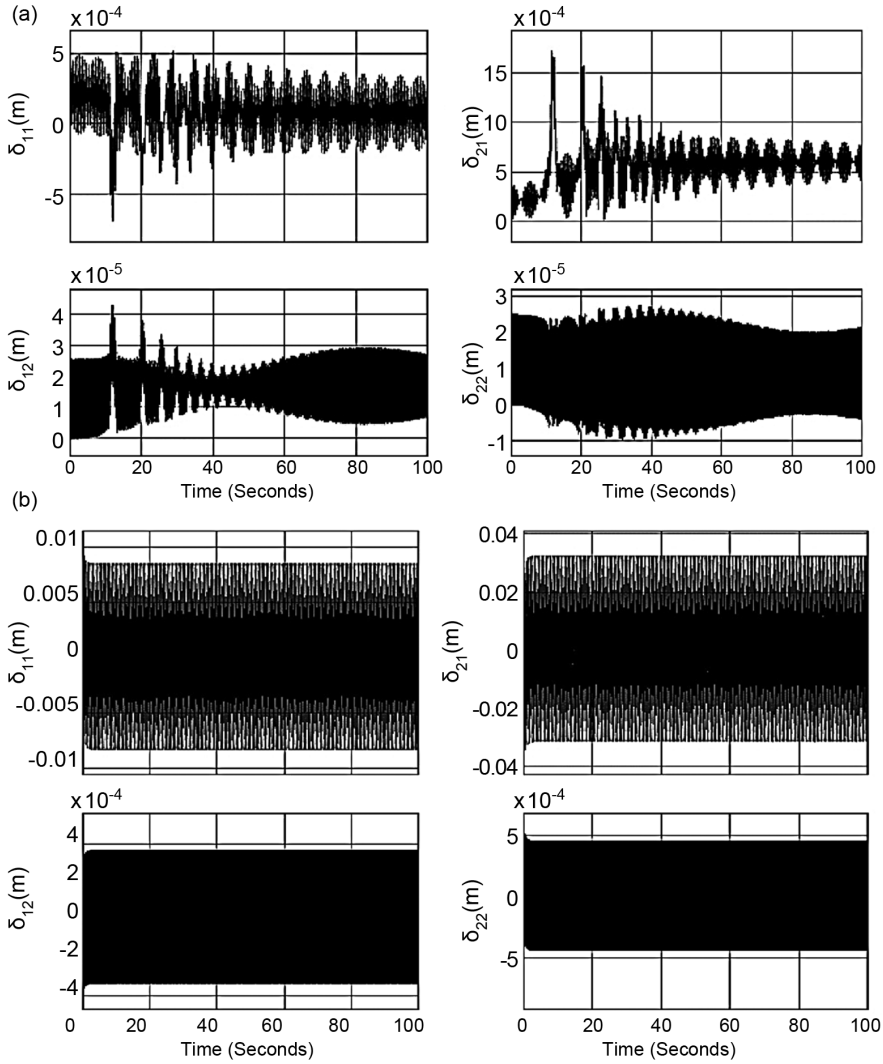

Fig. 5 — Modal function response, δ_{11} and δ_{12} are the modal function of Link 1 whereas δ_{21} and δ_{22} are the modal function of Link 2, when payload is $M_2 = 7$ *kg*; Results obtained using (a) Optimal robust controller and (b) Sliding mode controller

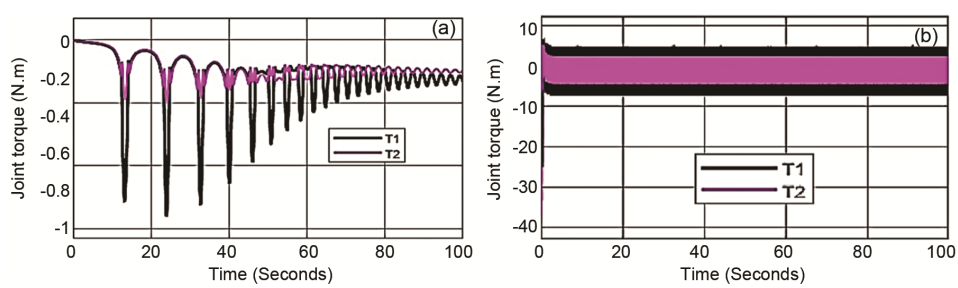

Fig. 6 — Control torque response of the joint actuators for M_2 = 10 *kg*; Results obtained using: (a) Optimal robust controller and (b) Sliding mode controller

uncertain parameter value set to 7 kg are shown in Figs 4 & 5, whereas that of 10 kg value are shown in Figs 6 & 7. It has been observed that the maximum amplitude of the deflection of the flexible links using the optimal robust controller is 10 times lesser compared to the link deflections obtained using the sliding mode controller. In the case of the sliding mode controller, the deflections of the links do not reduce but rather oscillate within a particular range, as shown in Figs 2–7. In the case of the optimal

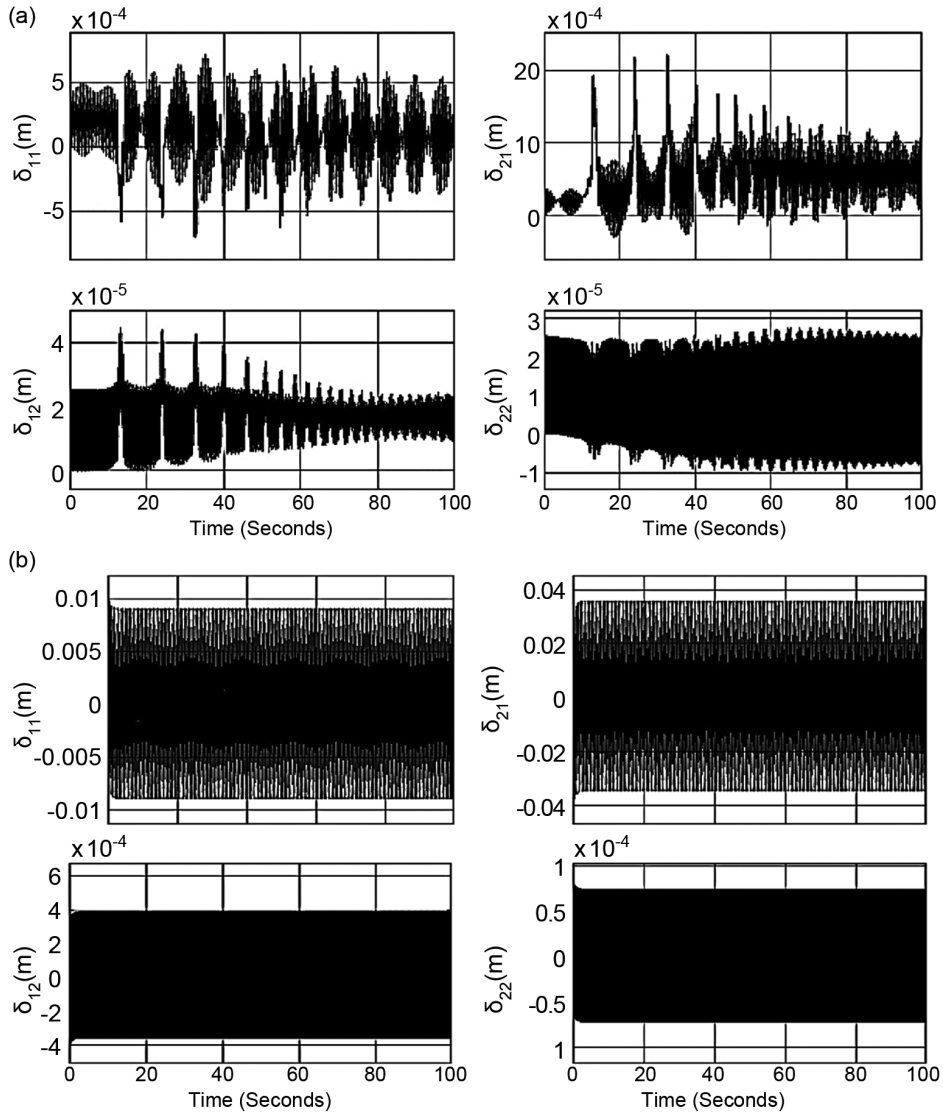

Fig. 7 — Modal function response, δ_{11} and δ_{12} are the modal function of Link 1 whereas δ_{21} and δ_{22} are the modal function of Link 2, when payload is $M_2 = 10$ *kg*; Results obtained using: (a) Optimal robust controller and (b) Sliding mode controller

Table 2 — Observation table

Controllers	Payload mass (kg)	Deflection (m)				Torque (N. m)	
	M_2	δ_{11max}	δ_{12max}	δ_{21max}	δ_{22max}	T_{1max}	T_{2max}
ORC	3 (Figs 2&3)	4.947×10^{-4}	3.023×10^{-5}	1.203×10^{-3}	2.916×10^{-5}	0.4179	0.1682
	7 (Figs 4&5)	6.952×10^{-4}	4.266×10^{-5}	1.718×10^{-3}	2.738×10^{-5}	0.9535	0.3496
	10 (Figs 6&7)	7.148×10^{-4}	4.466×10^{-5}	2.212×10^{-3}	2.751×10^{-5}	1.403	0.5092
SMC	3 (Figs 2&3)	7.255×10^{-3}	3.016×10^{-4}	2.367×10^{-2}	4.221×10^{-4}	4.722	4.848
	7 (Figs 4&5)	9.228×10^{-3}	4.623×10^{-4}	3.447×10^{-2}	7.571×10^{-4}	14.46	19.73
	10 (Figs 6&7)	9.819×10^{-3}	5.586×10^{-4}	3.758×10^{-2}	9.581×10^{-4}	25.08	37.54

robust controller, the link deflections are gradually reduced. To perform satisfactorily the maximum torque requirement of the designed Optimal Robust Controller (ORC) required very less compared to the Sliding Mode Controller (SMC) i.e., almost 10 times less (see Table 2). The entire process of the proposed methodology has been presented in Fig. 8.

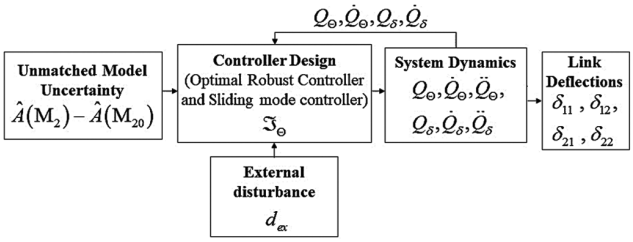

Fig. 8 — Work flow diagram

Conclusions

Considering external disturbance and unmatched model uncertainty, a specially designed Optimal Robust Controller (ORC) has been developed for TLFM. The proposed ORC eliminates the need for unknown gain terms, thus eliminating the requirement for additional tuning techniques to determine these values. Although the controllers were initially designed without considering external disturbances, they have demonstrated satisfactory performance even in the presence of such disturbances. The designed controller is fully equipped to handle various challenges encountered in this study, including link vibration, model uncertainty, and external disturbances, without any additional controllers or tuning methods. A comparative analysis clearly indicates the significant superiority of the ORC approach compared to the Sliding Mode Control (SMC) method, as evidenced by lower torque requirements and reduced deflection amplitudes. These findings indicate that the suggested ORC outperforms SMC in terms of performance. Furthermore, the proposed ORC methodology holds promise for application in other complex linear or nonlinear systems. Real-time implementation remains a potential future extension of this research.

Conflict of Interest

No potential conflicts of interest exist with regard to the research authoring, publication, or both of this work, the author has confirmed.

Acknowledgment

First Author expresses gratitude to NDF (AICTE) for providing financial support.

References

1 Lin F, *Robust control design: an optimal control approach* (John Wiley & Sons) 2007.

2 Hisseine D & Lohmann B, Robust control for a flexible-link manipulator using sliding mode techniques and nonlinear $\boldsymbol{H}_\infty$ design methods, *Proc ICRA IEEE Int Conf Robot Automat* (IEEE) 2001, 3865–3870, doi: 10.1109/ROBOT.2001.933220.

3 Karkoub M, Tamma K & Balas G, Robust control of two-link flexible manipulators using the μ-synthesis technique, *J Vib Control*, **5** (1999) 559–576, doi:10.1177/107754639900500404.

4 Li Y, Liu G, Hong T & Liu K, Robust control of a two-link flexible manipulator with neural networks based quasi-static deflection compensation, *Proc American Control Conf*, 6 (2003) 5258–5263, doi: 10.1109/ACC.2003.1242562.

5 Wang Z, Zeng H, Ho D W & Unbehauen H, Multi objective control of a four-link flexible manipulator: a robust $\boldsymbol{H}_\infty$ approach, *IEEE Trans Control Syst Technol*, **10** (2002) 866–875, doi: 10.1109/TCST.2002.804132.

6 Yang X, Ge S S & He W, Dynamic modeling and adaptive robust tracking control of a space robot with two-link flexible manipulators under unknown disturbances, *Int J Control*, **91** (2018) 969–988, doi: 10.1080/00207179.2017.1300837.

7 Daafouz J, Garcia G & Bernussou J, Robust control of a flexible robot arm using the quadratic d-stability approach, *IEEE Trans Control Syst Technol*, **6** (1998) 524–533, doi: 10.1109/87.701347.

8 Zhao Z, He X & Ahn C K, Boundary disturbance observer-based control of a vibrating single-link flexible manipulator, *IEEE Trans Syst Man Cybern: Syst*, **51** (2019) 2382–2390, doi: 10.1109/TSMC.2019.2912900.

9 Lochan K, Singh J P & Roy B K, Tracking control and deflection suppression of an AMM modelled TLFM using back stepping based adaptive SMC technique, in *Control Instrum Syst: Proc CISCON 2018* (Springer Singapore) 2020, 43–58, doi: 10.1007/978-981-13-9419-5_4.

10 Fayazi A, Pariz N, Karimpour A & Hosseinnia S H, Robust position-based impedance control of lightweight single-link flexible robots interacting with the unknown environment via a fractional-order sliding mode controller, *Robotica*, **36** (2018) 1920–1942, doi:10.1017/S0263574718000802.

11 Fareh R, Al-Shabi M, Bettayeb M & Ghommam J, Robust active disturbance rejection control for flexible link manipulator, *Robotica*, **38** (2020) 118–135, doi:10.1017/S026357471900050X.

12 Fayazi A, Pariz N, Karimpour A, Feliu-Batlle V & Hosseinnia S H, Adaptive sliding mode impedance control of single-link flexiblemanipulators interacting with the environment at an unknown intermediate point, *Robotica*, **38** (2020) 1642–1664, doi:10.1017/S026357471900167X.

13 Yu X, Hybrid-trajectory based terminal sliding mode control of a flexible space manipulator with an elastic base, *Robotica*, **38** (2020) 550–563, doi:10.1017/S0263574719000857.

14 Thakur S & Barai R K, "Joint trajectory tracking of two-link flexible manipulator in presence of matched uncertainty, *IEEE Int Conf Distrib Comput, VLSI, Elect Circuits Robotics* (IEEE) 2021, 151–154, doi: 10.1109/DISCOVER52564.2021.9663625.

15 Mohammadijoo A, Trajectory tracking of a 2-link mobile manipulator using sliding mode control method, *Int J Mech Mechatron Eng*, **17** (2023) 195–201, doi: 10.1109/DISCOVER52564.2021.9663625.

16 Mohamed Z, Khairudin M, Husain A & Subudhi B, Linear matrix inequality-based robust proportional derivative

control of a two-link flexible manipulator, *J Vib Control*, **22** (2016) 1244–1256, doi: 10.1177/1077546314536427.

17 Mahmood A, Moheimani S R & Bhikkaji B, Precise tip positioning of a flexible manipulator using resonant control, *IEEE/ASME Trans Mech*, **13** (2008) 180–186, doi: 10.1109/TMECH.2008.918494.

18 Pereira E, Aphale S S, Feliu V & Moheimani S R, Integral resonant control for vibration damping and precise tip-positioning of a single-link flexible manipulator, *IEEE/ASME Trans Mech*, **16** (2010) 232–240, doi: 10.1109/TMECH.2009.2039713.

19 Lee S H & Lee C W, Hybrid control scheme for robust tracking of two-link flexible manipulator, *J Intel Robot Syst*, **34** (2002) 431–452, doi: 10.1109/TMECH.2009.2039713.

20 Thakur S, Barai R K & Bhattacharya A, Trajectory tracking and link vibration reduction of flexible manipulator in the presence of matched uncertainty and external disturbances using lyapunov-based controller, *Adv Signal Process, Embedded Systems IoT: Proc Seventh* (Springer Nature Singapore) 2023, 543–552, doi: 10.1007/978-981-19-8865-3_49.

21 Sahu V S D M, Samal P & Panigrahi C K, Implementation of crow search algorithm for achieving optimal control of a single-link flexible manipulator, *Eng Technol Appl Sci Res*, 13 (2023) 9947–9954, doi: 10.48084/etasr.5385.

22 Sasaki M, Muguro J, Njeri W & Doss A S A, Adaptive notch filter in a two-link flexible manipulator for the compensation of vibration and gravity-induced distortion, *Vib*, 6 (2023) 286–302, doi: 10.3390/vibration6010018.

23 Abdul-Lateef W E, Alothman Y N I & Gitaffa S A H, An optimal motion path planning control of a robotic manipulator based on the hybrid PI-sliding mode controller, *Bulletin of Electrical Engineering and Informatics*, 12 (2023) 727–737, doi: 10.11591/eei.v12i2.3968.

24 Karkoub M, Balas G, Tamma K & Donath M, Robust control of flexible manipulators via μ-synthesis, *Control Eng Pract*, 8 (2000) 725–734, doi: 10.1016/S0967-0661(00)00006-X.

25 Morlock M, Bajrami V & Seifried R, Trajectory tracking with collision avoidance for a parallel robot with flexible links, *Control Eng Pract*, **111** (2021) 104788, doi: 10.1016/j.conengprac.2021.104788.

26 He W, Kang F, Kong L, Feng Y, Cheng G & Sun C, Vibration control of a constrained two-link flexible robotic manipulator with fixed-time convergence, *IEEE Trans Cybern*, **52(7)** (2021) 5973–5983. doi: 10.1109/TCYB. 2021.3064865.

27 Sayahkarajy M, Mode shape analysis, modal linearization, and control of an elastic two-link manipulator based on the normal modes, *Appl Math Model*, **59** (2018) 546–570, doi: 10.1016/j.apm.2018.02.003.

28 Yang X, Ge S S & He W, Dynamic modelling and adaptive robust tracking control of a space robot with two-link flexible manipulators under unknown disturbances, *Int J Control*, 91 (2018) 969–988, doi: 10.1080/00207179.2017. 1300837.

29 Ahmad M A, Mohamed Z, & Hambali N, Dynamic modelling of a two-link flexible manipulator system incorporating payload, *IEEE Conf Indust Electron Appl* (IEEE) 2008, 96–10, doi: 10.1109/ICIEA.2008. 4582487.

30 Mishra N & Singh S, Hybrid vibration control of a Two-Link Flexible manipulator, *App lSci*, 1 (2019) 715, doi: 10.1007/s42452-019-0691-1.

31 Wei C, Yueqing Y, Xuping Z & Liying S, Vibration controllability of under actuated robots with flexible links, *Int Technol Innov Conf* 2006, 1872–1878, doi: 10.1049/cp:20061072.

32 Qingsong C & Ailan Y, Optimal actuator placement for vibration control of two-link piezoelectric flexible manipulator, *Int Conf Mechanic Automat Control Eng* (IEEE) 2010, 2448–2451, doi: 10.1109/MACE.2010. 5535763.

33 Gao H, He W, Zhou C & Sun C, Neural network control of a two-link flexible robotic manipulator using assumed mode method, *IEEE Trans Ind Informat*, **15** (2018) 755–765, doi: 10.1109/TII.2018.2818120.

34 Huston R & Wang Y, Flexibility effects in multibody systems, in *Computer-aided Analysis of Rigid and Flexible Mechanical Systems*, 268 (1994) 351–376, doi: 10.1007/978-94-011-1166-9_11.

35 Giorgio & Vescovo D D, Non-linear lumped-parameter modeling of planar multi-link manipulators with highly flexible arms, *Robotics*, **7** (2018) 60, doi: 10.3390/robotics7040060.

36 Lochan K, Roy B & Subudhi B, SMC controlled chaotic trajectory tracking of two-link flexible manipulator with PID sliding surface, *IFAC-PapersOnLine*, 49 (2016) 219–224, doi: 10.1016/j.ifacol.2016.03.056.

37 Yang X & Zhong Z, Dynamics and terminal sliding mode control of two-link flexible manipulators with noncollocated feedback, *IFAC-PapersOnLine*, 46 (2013) 218–223, doi: 10.3182/20130902-3-CN-3020.00144.

38 Slotine J E & Li W, *Applied Nonlinear Control* (Prentice hall Englewood Cliffs, NJ) 1991.